

## ISOLATION AND CHARACTERIZATION OF RNA APTAMERS SPECIFIC FOR THE HUMAN TOLL-LIKE RECEPTOR 3 ECTODOMAIN

Tomoya Watanabe<sup>1</sup>, Kiyoharu Ito<sup>2</sup>, Misako Matsumoto<sup>2</sup>, Tsukasa Seya<sup>2</sup>, Kotomi Hatakeyama<sup>1</sup>, Satoshi Nishikawa<sup>3</sup>, Tsunemi Hasegawa<sup>1</sup>, and Kotaro Fukuda<sup>1\*</sup>

<sup>1</sup>Department of Material and Biological Chemistry, Faculty of Science, Yamagata University, Yamagata 990-8560, Japan.

\*Corresponding author: Kotaro Fukuda

FAX: 023-628-4604; E-mail: kotaro.f@sci.kj.yamagata-u.ac.jp

<sup>2</sup>Department of Microbiology and Immunology, Graduate School of Medicine, Hokkaido University, Sapporo 060-8638, Japan.

<sup>3</sup>Age Dimension Research Center, National Institute of Advanced Industrial Science and Technology (AIST), Tsukuba 305-8566, Japan.

(Received March 10, 2009; Accepted June 1, 2009)

### (Abstract)

Toll-like receptor 3 (TLR3) detects double-stranded RNA (dsRNA), known to be a universal viral molecular pattern, and activates the antiviral immune response. While TLR3 preferentially recognizes polyinosinic-polycytidylic acid (poly(I:C)), no sequence-specific dsRNA has been shown to activate TLR3. To determine whether TLR3 preferentially recognizes a specific RNA sequence or structure that acts upon the TLR3 signaling pathway, *in vitro* selection against the human TLR3 ectodomain (TLR3 ECD) was performed. After the seventh selection cycle, two major classes, Family-I and Family-II, emerged from 64 clones with binding constants of about 3 nM. To examine the structure–function relationship of Family-I and -II aptamers, mutational analyses and RNase mapping were carried out. Furthermore, to elucidate the effect of selected aptamers on TLR3 signaling *in vivo*, a reporter gene assay was conducted in cells. These aptamers did not have any agonistic or antagonistic effects on TLR3 signaling in TLR3-transfected HEK293 cells, although they bound to TLR3 ECD with high affinity *in vitro*. These results suggest that selection of RNA aptamers for TLR3 ECD should be performed under physiological conditions, since TLR3 ECD localizes in acidic compartments such as endosomes.

### (Keywords)

Toll-like receptor 3, TLR3 ectodomain, RNA aptamer, *in vitro* selection, SELEX

### 1. Introduction

Toll-like receptors (TLRs) play central roles in the innate immune response by recognizing conserved structural patterns in diverse microbial molecules [1]. All TLRs are type I integral membrane glycoproteins composed of an ectodomain (ECD) linked by a transmembrane domain to a cytoplasmic signaling Toll/IL-1 receptor (TIR) domain [2]. Ligand recognition by TLRs is mediated through their N-terminal ECD, which contains varying numbers of leucine-rich repeats (LRRs) [3]. More than 10 TLRs have been identified in human and mouse [4]. TLR1, TLR2, TLR4, TLR5, and TLR6 recognize bacterial cell wall and cell surface components, such as lipoproteins, lipopolysaccharide, and flagellin. In contrast, TLR3, TLR7, TLR8, and TLR9 recognize

pathogen nucleic acids, such as viral RNAs and bacterial DNA [4,5]. TLR3 recognizes double-stranded RNA (dsRNA) derived from viral genomes and replication intermediates and recruits TIR-containing adaptor molecule (TICAM)-I (also called TIR-containing adaptor inducing interferon (IFN)- $\beta$ , TRIF), leading to the production of IFN- $\beta$  and inflammatory cytokines [6,7]. As these immune responses are essential for combating viral invasions, TLR3 plays a key role in antiviral immunity. On the other hand, it is known that West Nile virus infection leads to a TLR3-dependent inflammatory response, which is involved in brain penetration of the virus and neuronal injury [8]. The three-dimensional structure of the human TLR3 ECD, which contains the dsRNA-binding region, has been reported by two groups [9,10]. TLR3 ECD resembles a horseshoe-shaped solenoid of 23 LRRs, with each LRR forming one turn of the solenoid. Furthermore, a recent report revealed the crystal structure of TLR3 ECD bound to a dsRNA ligand [11]. Each TLR3 ECD binds to a dsRNA at two sites located at opposite ends of the TLR3 horseshoe, and an intermolecular interaction between the two TLR3 ECD C-terminal domains coordinates and stabilizes the dimer formation.

Nucleic acid-sensing TLRs, TLR3, TLR7, TLR8, and TLR9, are localized in the endosome [12,13]. It has been reported that TLR7 and TLR8 (receptors for single-stranded RNA), as well as TLR9 (a receptor for CpG oligodeoxyribonucleotide), respond to their ligands in a sequence-dependent manner [14]. Although polyinosinic-polycytidylic acid (poly(I:C)), a synthetic dsRNA analogue, is a potent inducer of TLR3 signaling, no sequence-specific inducer or inhibitor for TLR3 is known. Anti-inflammatory drugs (TLR3 antagonists) and adjuvants for vaccines (TLR3 agonists) that regulate TLR3 signal transduction could be important for the development of future therapeutic treatments. Therefore, to investigate whether TLR3 recognizes and responds to specific dsRNA, *in vitro* selection against TLR3 ECD was carried out. *In vitro* selection (SELEX) is a powerful tool for obtaining RNA ligands that bind to a target molecule with high affinity and specificity [15,16]. So far, high-affinity DNA or RNA ligands for target molecules including proteins, organic dyes, and amino acids have been isolated by *in vitro* selection [17]. Because binding of

an aptamer to its target is a highly specific interaction that involves discrimination between related proteins that share common sets of structural domains, aptamers represent a potentially attractive class of molecules for therapeutic compounds. Furthermore, RNA aptamers against RNA-binding proteins (RBPs) are useful for dissecting the interactions between RNA and protein, and such aptamers could potentially modulate the function of target RBPs.

This report describes the isolation and characterization of RNA aptamers that bind with high specificity to human TLR3 ECD. Application of TLR3 ECD aptamers *in vivo* is also described to estimate their agonistic and antagonistic effects on TLR3 signaling.

## 2. Materials and Methods

### 2.1. Protein and nucleic acids

TLR3 ECD with an N-terminal FLAG tag and C-terminal His tag (TLR3-ECD) was expressed using a baculovirus system and purified as described previously [18]. The starting RNA pool of N40H for *in vitro* selection has the sequence 5'-GGUAGAUACGAUGGA-(N40)-CAUGACGCG CAGCCA-3'. The antisense DNA template, 5'-TGGCTGCGCGTCATG-(N40)-TCCATCGTATC TACC-3' (10 pmol), was converted to dsDNA by PCR with a 5'-end primer, 5'-TGTAATACGACTCACTATAGGTAGATACGAT GGA-3' (40 pmol). Underlined letters in the 5'-end primer indicate the T7 RNA promoter sequence. PCR was carried out for six cycles, and dsDNA was recovered by ethanol precipitation. The dsDNA (50 pmol) was reamplified by PCR with the 5'-end primer and a 3'-end primer, 5'-TGGCTGCGCGTCATG -3' (100 pmol each). After 20 cycles of PCR, the amplified DNA pool was recovered by ethanol precipitation. T7 RNA transcription was performed with at least 100 pmol of the DNA pool using the T7 AmpliScribe Kit (Epicentre Technologies). The transcribed RNA was then purified on 8% denaturing

PAGE. The final yield of the random RNA pool N40H was approximately 70 µg.

Family-I and -II aptamer mutants were constructed by PCR mutagenesis using mutagenic primers and template DNA. The DNA sequences of these mutants were confirmed by an Applied Biosystems model 3100 automatic sequencer (Applied Biosystems).

### 2.2. *In vitro* selection of RNA aptamers for TLR3-ECD

*In vitro* selection was carried out essentially as reported previously [19]. For the first cycle of selection, the N40H RNA pool (500 pmol) was incubated with 62.5 pmol of TLR-ECD in 50 µl of binding buffer [2 mM HEPES-NaOH (pH 7.6), 3 mM MgCl<sub>2</sub>, and 100 mM NaCl] at room temperature for 1 h. The binding reaction was separated by filtration through a nitrocellulose filter (HAWP filter, 0.45 µm) fitted in a pop-top filter holder (Nucleopore) and washed with 1 mL of binding buffer. The filter was eluted with 200 µl of elution buffer [0.4 M sodium acetate (pH 5.5), 5 mM EDTA (pH 8.0), and 7 M urea] at 90°C for 5 min. The eluted RNA was recovered by ethanol precipitation and reverse-transcribed using RevertAid™ M-MuLV Reverse Transcriptase (Fermentas) at 42°C for 1 h. The cDNA product was amplified by PCR and transcribed *in vitro* using the T7 AmpliScribe Kit (Epicentre Technologies). The product of this reaction was subjected to another cycle of selection for a total of 10 cycles. To specifically enrich the RNA pool for high-affinity ligands for TLR-ECD, the concentration of TLR-ECD and the RNA ligand were manipulated for each selection cycle (Table 1). Yeast tRNA (Boehringer Mannheim) was used as a non-specific competitor during the selection process.

The PCR product of the seventh selection cycle was introduced into the TA cloning vector (Invitrogen). After subcloning and transformation into *E. coli*, plasmid DNA was isolated from

Table 1. TLR3-ECD aptamer selection and binding analysis. TLR3-ECD, RNA pool, and competitor tRNA concentrations used during the selection step (total volume, 50 µL) of each generation are shown. The binding activity of the RNA pool at each cycle was analyzed by a filter binding assay with competitor tRNA (TLR3-ECD : RNA pool: tRNA = 0.05 : 0.05 : 2.5 µM) as described in the Materials and Methods. Binding activities were calculated as the percent of input RNA.

Generation No.	Concentration (µM)			Binding (%)
	TLR3-ECD protein	RNA pool	Competitor tRNA	
1	1.25	10.0	0.0	0
2	0.625	5.0	2.5	0.1
3	0.3	2.4	4.8	0
4	0.3	2.4	12.0	0.9
5	0.15	1.5	12.0	8.9
6	0.075	0.75	12.0	13.1
7	0.05	0.5	10.0	17
8	0.025	0.25	6.25	16
9	0.025	0.25	7.5	15
10	0.012	0.12	4.2	14

individual clones and the DNA sequences of 64 clones were analyzed with an Applied Biosystems model 3100 automatic sequencer (Applied Biosystems). The secondary structure models of selected aptamers, Family-I and -II, were drawn by the Mulfold program based on the Zuker algorithm [20].

### 2.3. Filter binding assay

The binding activity of the RNA pool was analyzed after each selection cycle. PCR products were internally transcribed *in vitro* with [ $\alpha$ - $^{32}$ P]CTP (Amersham), and the transcription product was tested by a filter binding assay using equimolar TLR-ECD and RNA and a 50-fold molar excess of non-specific competitor tRNA (TLR-ECD and RNA pool, 50 nM; tRNA, 2.5  $\mu$ M) in binding buffer [2 mM HEPES-NaOH (pH 7.6), 3 mM MgCl<sub>2</sub>, and 100 mM NaCl]. Radioactivity retained on the filter was counted with a BAS2000 image analyzer (Fuji Film). The binding activity was evaluated by calculating the percent of the input RNA retained on the filter in complexes with TLR-ECD (Table 1).

The equilibrium dissociation constants ( $K_D$ ) for the selected aptamers, Family-I and -II, were determined by using a constant amount of internally labeled RNA aptamer (1 nM) in binding reactions with increasing concentrations of TLR-ECD (0.25–64 nM). Mixtures containing RNA and TLR-ECD were passed through a nitrocellulose filter and the filter was washed with 1 mL of binding buffer. The data points were fitted to a Scatchard plot to determine the equilibrium dissociation constant by Prism 4 ver 4.0b (GraphPad Software Inc.).

To analyze the binding ability of Family-I and -II mutants to TLR3-ECD, each  $^{32}$ P-labeled mutant RNA (50 nM) was incubated with TLR3-ECD (50 nM) in 50  $\mu$ l of binding buffer at 37°C for 1 h. The protein/RNA complex was separated by filtration on a nitrocellulose filter as described above. Radioactivity remaining on the filter was measured using a BAS2000 image analyzer (FujiFilm), and the amount of Family-I and -II mutants bound to TLR3-ECD was calculated as a percentage of the RNA input prior to filtration.

### 2.4. Structural analysis of RNA aptamers

For enzymatic probing, 5'-end-labeled Family-I and -II were partially digested with RNases T1 or A as previously reported with slight modifications [19], and the cleaved products were analyzed by 12% PAGE (7 M urea) with alkaline ladder of Family-I and -II.

### 2.5. Cell culture

For the expression of plasmids encoding human TLR3, HEK293 (human embryonic kidney) cells were used and cultured in DMEM cell culture medium (GIBCO) supplemented with 10% heat-inactivated fetal bovine serum (BIOSOURCE) and antibiotics (penicillin/streptomycin).

### 2.6. Reporter gene assay

HEK293 cells were seeded in 24-well plates (5  $\times$  10<sup>5</sup> cells/well). Twenty-four hours later, the cells were transiently transfected with pEFBOS/TLR3 (0.1  $\mu$ g) together with a p125-luc reporter (0.1  $\mu$ g) and Renilla luciferase reporter (2.5 ng) in the presence of Lipofectamine 2000 (Invitrogen). The total amount of transfected plasmid (0.8  $\mu$ g) was kept constant by adding empty vector. Twenty-four hours after transfection, the medium was replaced by fresh medium. RNA aptamer, poly(I:C) or both, was mixed with DOTAP Liposomal Transfection Reagent (3  $\mu$ g/well; Roche) in OPTI-MEM (7  $\mu$ l/well; Invitrogen) and pre-incubated for 15 min at R.T. The DOTAP/RNA complex was then transfected into cells and incubated. Cells were collected and washed twice with 1 ml of PBS buffer. The collected cells were then lysed using Passive Lysis Buffer (Promega), and the cell lysates were assayed for the dual luciferase activities (Promega). Data are expressed as mean relative stimulation SD for a representative experiment from independent experiments, performed in duplicate.

## 3. Results

### 3.1. Sequence and secondary structure of RNA aptamers specific for TLR3 ECD

To isolate high-affinity RNA ligands for TLR3 ECD, *in vitro* selection was carried out using an RNA library containing N40 random core sequences and recombinant TLR3-ECD protein. Initially, the randomized RNA pool (N40H), which consists of approximately 3  $\times$  10<sup>14</sup> molecules (500 pmol), was incubated with TLR3-ECD (62.5 pmol), and the RNA/TLR3-ECD complexes were separated from the unbound RNA molecules by passage through a nitrocellulose filter. The RNA retained on the filter was recovered, subjected to RT-PCR, transcribed by T7 RNA polymerase, and used for the next selection cycle. To specifically enrich the RNA pool for high-affinity ligands specific for TLR3-ECD, the concentrations of TLR3-ECD, RNA ligand, and competitor tRNA were manipulated for each selection cycle (Table 1). To confirm whether the selected RNA pools bind to TLR3-ECD, the binding activity of the RNA pools was evaluated by a filter binding assay after each selection cycle. The RNA pool from the seventh selection cycle (G7) had the highest affinity; about 17% of the total RNA pool bound to TLR3-ECD (Table 1).

To analyze the sequence and structural motifs in the G7 pool, we cloned the seventh-cycle PCR product into the TA vector and sequenced 64 clones. Although there were no conserved sequences among any of the clones, we were able to categorize them into 11 classes, from Family-I to -XI as shown in Table 2. Of these, two major classes emerged with entirely identical sequences: Family-I with 12 clones, followed by Family-II with 11 clones. We therefore focused on these Family-I and -II aptamers and proceeded to characterize them. When the secondary structures of the two aptamer classes were analyzed by the Mulfold program [20], we found that both

Table 2. Nucleotides sequences of RNA aptamers categorized into Family-I – Family-XI. Selected sequences from the G7 RNA pool are shown in uppercase. The fixed sequences for PCR primers are indicated in lowercase. Numbers in parentheses indicate the number of identical clones.

<b>Family-I (12)</b>	<b>gguagauacgau</b> gga UCAGGGUACCCCCUGUGGCCCGUCAACACAGGGGAAGUGG <b>caugacgcgcagcca</b>
<b>Family-II (11)</b>	<b>gguagauacgau</b> gga CUACCGCCACCCCGGGUCCGGUGACGUUAAUUGAGGGCC <b>caugacgcgcagcca</b>
<b>Family-III (4)</b>	<b>gguagauacgau</b> gga ACAUGCCGGCAGGUGAGGCUGCACCUGUCUUUAAGGCGU <b>caugacgcgcagcca</b>
<b>Family-IV (4)</b>	<b>gguagauacgau</b> gga CCGGUCCCAGCGUUCAAGAGACCGGGGCGAGCAAGCAGU <b>caugacgcgcagcca</b>
<b>Family-V (3)</b>	<b>gguagauacgau</b> gga GGCAGCGAGGUGAAGCUGTAGUUAAGAAGACCAACAGG <b>caugacgcgcagcca</b>
<b>Family-VI (3)</b>	<b>gguagauacgau</b> gga ACAAGAAUGGGCCCCGAGGUUCGUCAGCUGGGGGCAAGGG <b>caugacgcgcagcca</b>
<b>Family-VII (3)</b>	<b>gguagauacgau</b> gga CGGACGACCAUUGUCGAAGUAACCGUCGUCCGAAGCUGGC <b>caugacgcgcagcca</b>
<b>Family-VIII (2)</b>	<b>gguagauacgau</b> gga CGGAUCGUUCGCUCCCAGAAAGCGCGACUCUGAGGUUAAG <b>caugacgcgcagcca</b>
<b>Family-IX (2)</b>	<b>gguagauacgau</b> gga UACACAGCCGGCAGACGCGCUGUCGUUAACGCAGGC GAAA <b>caugacgcgcagcca</b>
<b>Family-X (2)</b>	<b>gguagauacgau</b> gga CCACAAAACCCGGCAGUCGGUGAGCAGGCCACGAUCGGC <b>caugacgcgcagcca</b>
<b>Family-XI (2)</b>	<b>gguagauacgau</b> gga UCAACAACAACA AAUACAAGGCCCGUGCTACCGCGAAG <b>caugacgcgcagcca</b>
<b>Others (16)</b>	<b>Orphan sequence</b>

Family-I and -II aptamers were composed of three stem-loop (SL) structures, but we did not observe any sequence conservation or structural similarity between the two Families (Fig. 1).

### 3.2. Binding activity of Family-I and -II aptamers to TLR3 ECD

The equilibrium dissociation constant ( $K_D$ ) of Family-I and -II aptamers was determined by a filter binding assay. Each aptamer (1 nM) was internally labeled and incubated with increasing concentrations of TLR3-ECD (0.25–64 nM) in the binding buffer. When the molar ratio of the RNA aptamers and TLR3-ECD was 1:64 (1 nM : 64 nM), approximately 27% maximal binding activity was observed (Fig. 2). The data points were fitted to a Scatchard plot to determine the equilibrium dissociation constant using Prism 4 ver 4.0b (GraphPad Software Inc.). The apparent  $K_D$  values for the aptamers were approximately 3 nM (Family-I, 2.1 nM; Family-II, 3.6 nM). Based on the  $K_D$  values for TLR3-ECD, selected Family-I and -II aptamers harbor high affinity for TLR3-ECD.

### 3.3. Enzymatic probing of Family-I and -II aptamers

The secondary structure models for Family-I and -II aptamers shown in Fig. 1 are based on Mulfold analysis of the RNA sequences. To confirm whether the solution structures of the two aptamer groups are consistent with the proposed secondary structure models, Family-I and -II aptamers were subjected to enzymatic probing using RNases T1 and A, which cleave adjacent to the 3'-phosphate of G

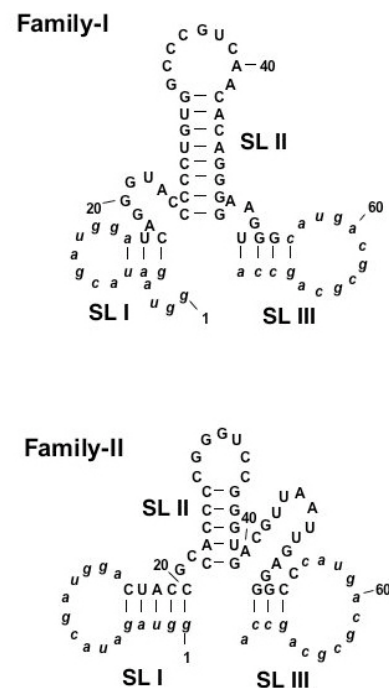


Figure 1. The secondary structure models of Family-I and -II aptamers against TLR3-ECD predicted by the Mulfold program [20]. Selected sequences are shown in normal letters. Lowercase letters indicate the constant sequence regions flanking the randomized N40 core. SL, stem-loop structure.

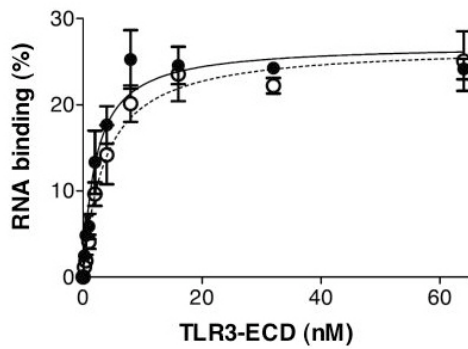


Figure 2. Binding curves of Family-I and -II aptamers for TLR3-ECD. Data points were obtained by a filter binding assay (50  $\mu$ l reaction) as described in the Materials and Methods (Family-I, closed circles with solid line; Family-II, open circles with dotted line). The concentration of labeled aptamers was 1 nM. The values represent means of three independent experiments. RNA binding shows the percentage of RNA retained on the filter in protein/RNA complex against input RNA.

and pyrimidine nucleotides, respectively. 5'-end-labeled Family-I and -II RNAs were partially digested, and the cleavage products were analyzed by denaturing 12% PAGE (Fig. 3A and 3C). The secondary structures of the Family-I and -II aptamers, cleavage sites were observed mainly at unpaired residues, corresponding to loop regions and spacer sequences flanked by stem-loop structures (Fig. 3B and 3D). In general, the cleavage patterns of the two enzymes appear to be consistent with the proposed

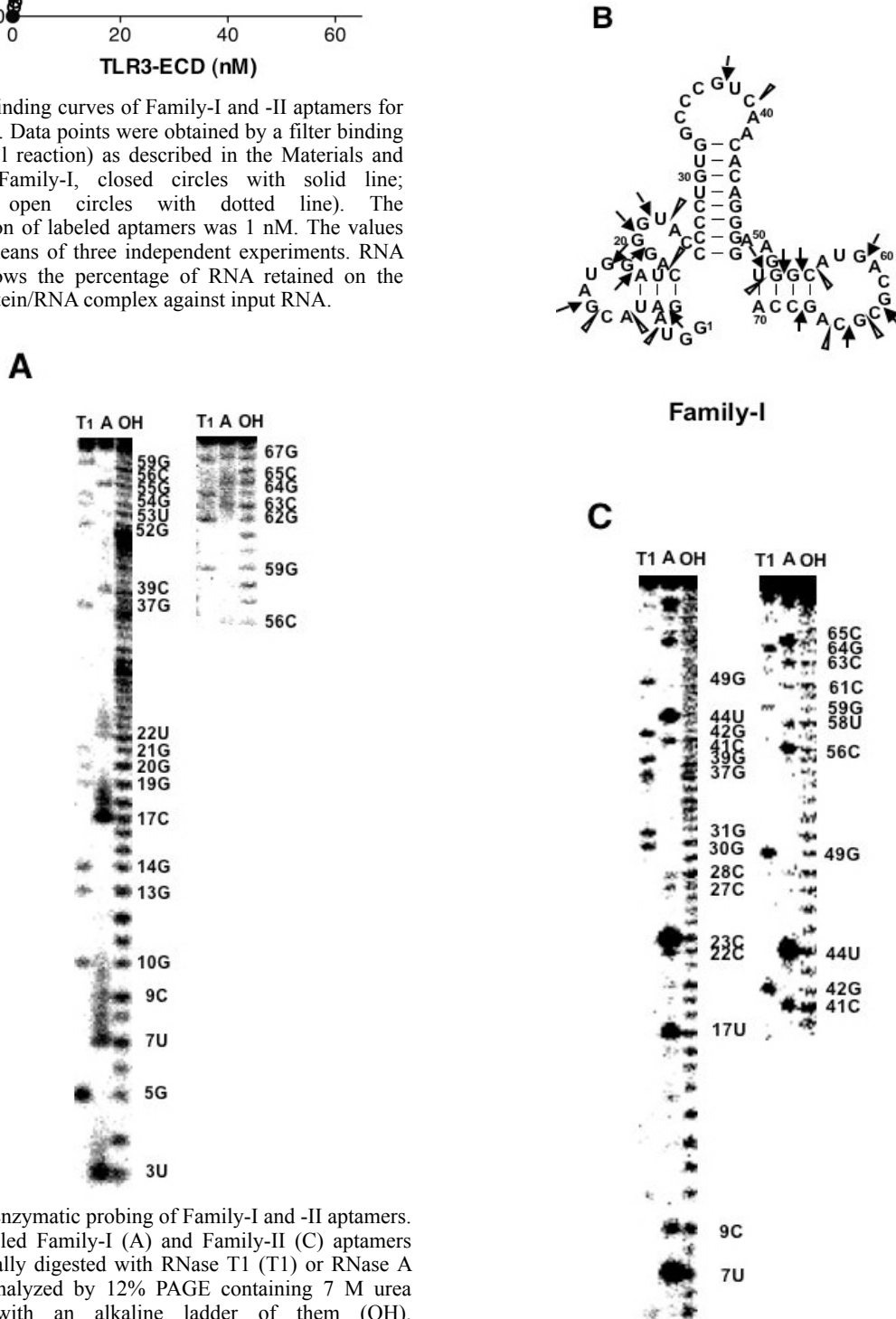


Figure 3. Enzymatic probing of Family-I and -II aptamers. 5'-end-labeled Family-I (A) and Family-II (C) aptamers were partially digested with RNase T1 (T1) or RNase A (A) and analyzed by 12% PAGE containing 7 M urea together with an alkaline ladder of them (OH). Nuclease-accessible sites in Family-I (B) and in Family-II (D) aptamers are shown by arrows (RNase T1) and open triangles (RNase A), respectively.



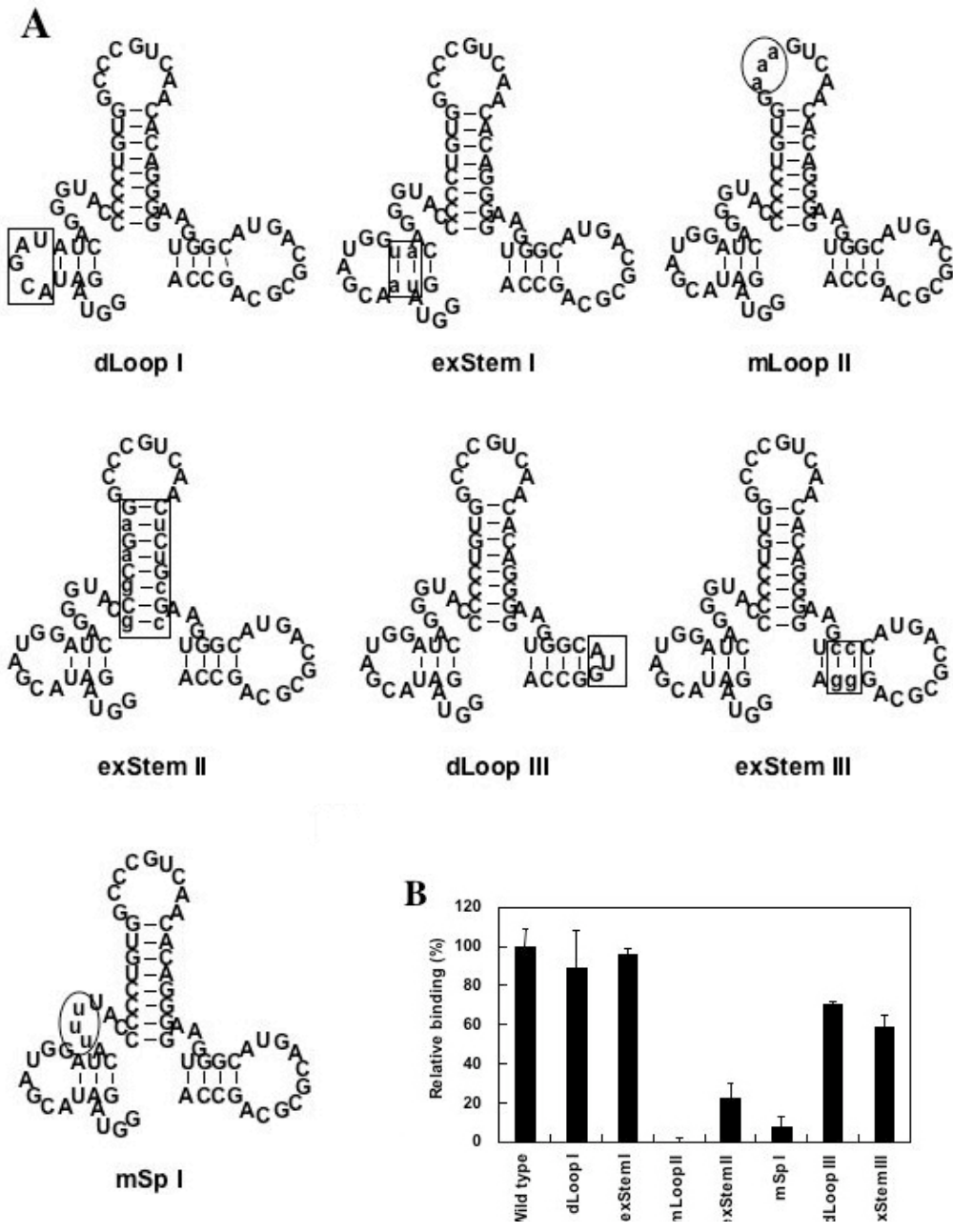


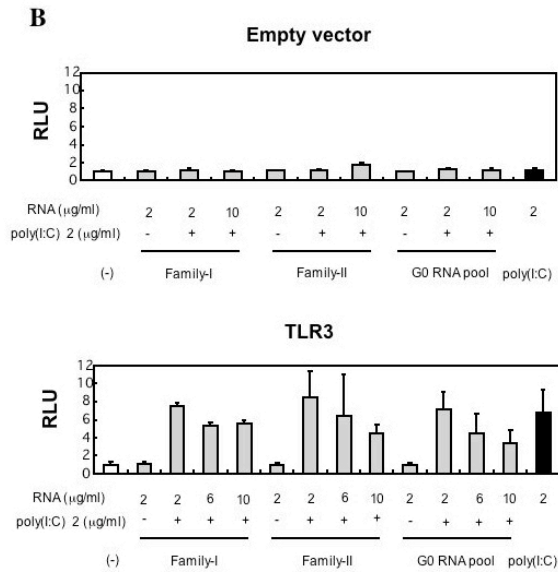
Figure 4. Binding analyses of Family-I and -II aptamer mutants to TLR3-ECD. Secondary structures of mutants in Family-I (A) and -II aptamers (C) are shown. Mutated regions are circled and boxed; small letters indicate the exchanged or introduced bases. The binding activity of Family-I (B) and -II (D) aptamer mutants were examined by a filter binding assay as described in the Materials and Methods. The values represent the means of three independent experiments and the relative RNA binding activity (wild type=100%) shows the percentage of RNA retained on the filter in protein/RNA complex against input RNA.

sequence-specific inducer, or inhibitor, has not been identified.

It is important to develop novel RNAs that function as anti-inflammatory drugs (TLR3 antagonists) and adjuvants for vaccines (TLR3 agonists). For this purpose, *in vitro* selection against TLR3 ECD was performed using a recombinant TLR3-ECD protein and a synthetic N40 random RNA pool. We succeeded in obtaining two classes of

RNA aptamers specific for TLR3-ECD, designated as Family-I and -II. Although both show high affinity for the target with  $K_D$  values of about 2 to 4 nM, they do not harbor any conserved sequences between them. Mutational analyses on Family-I and -II aptamers revealed that particular regions, such as SL II structures and spacer sequences, are indispensable for binding to TLR3-ECD. The binding site of the selected RNA aptamers on TLR3 ECD is not known,





speculation is supported by the results, which showed that Family-I and -II aptamers mimicked the antagonistic effect as observed in the G0 RNA pool (Fig. 5B). In addition, the length of the double-stranded region of the RNA is also important for binding to TLR3 [21, 25]. Therefore, the binding region of the RNA aptamers may be too short, or their binding may not be specific to the functional regions of TLR3 ECD for proper signaling. Furthermore, steric hindrance by higher structure glycosylation, or the presence of co-receptors, or accessory molecules, may affect the precise interaction of ligands.

In this study, we obtained RNA aptamers (Family-I and -II) that bind to TLR3 ECD with high affinity. These aptamers showed neither agonistic, nor antagonistic effects on TLR3 signaling in a cell-based assay. However, the function of TLR3 might be manipulated by designing novel RNA constructs based on these two aptamers, or a new *in vitro* selection procedure under acidic conditions could create functional aptamers that regulate TLR3 signaling *in vivo*.

### Acknowledgement

We thank T. Tokisue for helpful discussions.

### References

1. Takeda, K., Kaisho, T., and Akira, S. Toll-like receptors, *Annu. Rev. Immunol.* 21, 335-376 (2003).
2. Gay, N. J., and Gangloff, M. Structure and function of Toll receptors and their ligands, *Annu. Rev. Biochem.* 76, 141-165 (2007).
3. Medzhitov, R. Toll-like receptors and innate immunity, *Nat. Rev. Immunol.* 1, 135-145 (2001).
4. O'Neill, L. A. TLRs: Professor Mechnikov, sit on your hat, *Trends Immunol.* 25, 687-693 (2004).
5. Akira, S., and Takeda, K. Toll-like receptor signaling, *Nat. Rev. Immunol.* 4, 499-511 (2004).

6. Alexopoulou, L., Holt, A. C., Medzhitov, R., and Flavell, R. A. Recognition of double-stranded RNA and activation of NF- $\kappa$ B by Toll-like receptor 3, *Nature* 413, 732-738 (2001).
7. Oshiumi, H., Matsumoto, M., Funami, K., Akazawa, T., and Seya, T. TICAM-1, an adaptor molecule that participates in Toll-like receptor 3-mediated interferon- $\beta$  induction, *Nat. Immunol.* 4, 161-167 (2003).
8. Wang, T., Town, T., Alexopoulou, L., Anderson, J. F., Fikrig, E., and Flavell, R. A. Toll-like receptor 3 mediates West Nile virus entry into the brain causing lethal encephalitis, *Nat. Med.* 10, 1366-1373 (2004).
9. Choe, J., Kelker, M. S., and Wilson, I. A. Crystal structure of human Toll-like receptor 3 (TLR3) ectodomain, *Science* 309, 581-585 (2005).
10. Bell, J. K., Botos, I., Hall, P. R., Askins, J., Shiloach, J., Segal, D. M., and Davies, D. R. The molecular structure of the Toll-like receptor 3 ligand-binding domain, *Proc. Natl. Acad. Sci. U. S. A.* 102, 10976-10980 (2005).
11. Liu, L., Botos, I., Wang, Y., Leonard, J. N., Shiloach, J., Segal, D. M., and Davies, D. R. Structural basis of Toll-like receptor 3 signaling with double-stranded RNA, *Science* 320, 379-381 (2008).
12. Matsumoto, M., Funami, K., Tanabe, M., Oshiumi, H., Shingai, M., Seto, Y., Yamamoto, A., and Seya, T. Subcellular localization of Toll-like receptor 3 in human dendritic cells, *J. Immunol.* 171, 3154-3162 (2003).
13. Kawai, T., and Akira, S. Antiviral signaling through pattern recognition receptors, *J. Biochem.* 141, 137-145 (2007).
14. Marques, J. T., and Williams, B. R. Activation of the mammalian immune system by siRNAs, *Nat. biotechnol.* 23, 1399-1405 (2005).
15. Ellington, A. D., and Szostak, J. W. *In vitro* selection of RNA molecules that bind specific ligands, *Nature* 346, 818-822 (1990).
16. Tuerk, C., and Gold, L. Systematic evolution of ligands by exponential enrichment: RNA ligands to bacteriophage T4 DNA polymerase, *Science* 249, 505-510 (1990).
17. Tuerk, C. Using the SELEX combinatorial chemistry process to find high affinity nucleic acid ligands to target molecules, *Methods Mol. Biol.* 67, 219-230 (1997).
18. Fukuda, K., Watanabe, T., Tokisue, T., Tsujita, T., Nishikawa, S., Hasegawa, T., Seya, T., and Matsumoto, M. Modulation of double-stranded RNA recognition by the N-terminal histidine-rich region of the human Toll-like receptor 3, *J. Biol. Chem.* 283, 22787-22794 (2008).
19. Fukuda, K., Vishnuvardhan, D., Sekiya, S., Hwang, J., Kakiuchi, N., Taira, K., Shimotohno, K., Kumar, P. K., and Nishikawa, S. Isolation and characterization of RNA aptamers specific for the hepatitis C virus nonstructural protein 3 protease, *Eur. J. Biochem.* 267, 3685-3694 (2000).
20. Zuker, M. Computer prediction of RNA structure, *Methods Enzymol.* 180, 262-288 (1989).
21. Okahira, S., Nishikawa, F., Nishikawa, S., Akazawa, T., Seya, T., and Matsumoto, M. Interferon- $\beta$  induction through Toll-like receptor 3 depends on double-stranded RNA structure, *DNA Cell Biol.* 24, 614-623 (2005).
22. Matsumoto, M., and Seya, T. TLR3: interferon induction by double-stranded RNA including poly(I:C), *Advanced Drug Delivery Reviews* 60, 805-812 (2008).
23. de Bouteiller, O., Merck, E., Hasan, U. A., Hubac, S., Benguigui, B., Trinchieri, G., Bates, E. E., and Caux, C. Recognition of double-stranded RNA by human Toll-like receptor 3 and downstream receptor signaling requires multimerization and an acidic pH, *J. Biol. Chem.* 280, 38133-38145 (2005).
24. Bell, J. K., Askins, J., Hall, P. R., Davies, D. R., and Segal, D. M. The dsRNA binding site of human Toll-like receptor 3, *Proc. Natl. Acad. Sci. U. S. A.* 103, 8792-8797 (2006).
25. Leonard, J. N., Ghirlando, R., Askins, J., Bell, J. K., Margulies, D. H., Davies, D. R., and Segal, D. M. The TLR3 signaling complex forms by cooperative receptor dimerization, *Proc. Natl. Acad. Sci. U. S. A.* 105, 258-263 (2008).